Quantifying Fibrosis in Venous Disease: Mechanical Properties of Lipodermatosclerotic and Healthy Tissue

Mary Jo Geyer, PhD, PT; David M. Brienza, PhD; Vikram Chib, MS; and Jue Wang, PhD

ABSTRACT

OBJECTIVES: To quantify the mechanical properties of medioposterior bulk calf tissue in patients with lipodermatosclerotic venous-insufficient tissue and individuals with apparently healthy tissue using a novel ultrasound indentometry method, and to identify parameters with the potential for quantifying fibrosis in subsequent studies.

DESIGN: 2-group, quasi-experimental design

SETTING: Soft Tissue Mechanics Laboratory, University of Pittsburgh, Pittsburgh, PA

PARTICIPANTS: 9 healthy and 9 venous-insufficient individuals aged 35 to 85 years

INTERVENTIONS: Ultrasound indentometry and computed tomography (CT) of calf tissue

MAIN OUTCOME MEASURES: Between group differences and associations among quasi-linear viscoelastic (QLV) tissue parameters and CT descriptors

MAIN RESULTS: Established the accuracy, validity, and reliability of the QLV model and ultrasound indentometry method. Demonstrated a range of significant differences between the groups (P <.020 to P <.004) for selected QLV parameters. Also found significant correlations between CT measures of fibrosis and dermal thickness and QLV elastic measures (P <.034 to P <.005).

CONCLUSION: Attempts to quantify fibrosis in lipodermatosclerosis have included histologic exams, palpation/pitting, durometer readings, and imaging techniques, but these efforts have failed to produce a clinically practical, noninvasive method. A novel ultrasound indentometry method was used to acquire in vivo data from which tissue parameters were derived. These data support the further development of ultrasound indentometry as a method to quantify fibrosis in venous disease.

ADV SKIN WOUND CARE 2004;17:131-42.

Management of venous disease has become a major health care challenge. Characterized by chronicity and relapse, venous disease management commonly leads to massive expenditures in developed countries. In the United States alone, this expenditure is estimated at $2 to $4 billion per year, with 200 million lost work days per year.[1-3] The magnitude of these expenditures in conjunction with the relative lack of treatments demonstrating long-term effectiveness has stimulated renewed interest in research on venous disease. One aspect of such research has focused on the measurement of fibrotic soft tissue changes that occur almost universally with severe chronic venous disease. This progressive hardening of the skin and subcutaneous tissue is known as lipodermatosclerosis (LDS)[4-8] (Figure 1).

Fibrosis is the primary distinguishing characteristic of LDS. Evidence suggests that the ability to accurately quantify tissue fibrosis would aid in the early detection, differential diagnosis, staging, and classification of venous disease, as well as in the

Mary Jo Geyer, PhD, PT, is Director of Lymphedema and Wound Care Clinical Support Services and Research, VA Pittsburgh Healthcare System, Pittsburgh, PA. David M. Brienza, PhD, is Associate Professor and Director, Soft Tissue Mechanics Laboratory, Rehabilitation Science and Technology Department, School of Health and Rehabilitation Sciences, University of Pittsburgh, Pittsburgh, PA. Vikram S. Chib, MS, is a doctoral student in biomedical engineering, Northwestern University, Chicago, IL. Jue Wang, PhD, is Professor and Director, Research Center of Rehabilitation Sciences and Technology, School of Life Science and Technology, Xi'an Jiaotong University, Xi'an, Shaanxi, 710049, P.R. of China.

ACKNOWLEDGMENTS The authors thank the Soft Tissue Mechanics Laboratory, Department of Rehabilitation Science and Technology, University of Pittsburgh, for funding this project. Additional thanks to the following individuals and organizations for their expertise and in-kind support of this project: Bertan Ozgun, MD, Advanced Radiology, PC, Baltimore, MD; David L. Steed, MD, Director, Wound Healing and Limb Preservation Clinic, University of Pittsburgh Medical Center, Pittsburgh, PA; Ray G. Burdett, PhD, PT, Assistant Dean, Undergraduate Programs in Rehabilitation Science, School of Health and Rehabilitation Sciences University of Pittsburgh; Mike Grguras, Valencia, PA; Biersdorf-Jobst, Inc, Charlotte, NC; and Medical Center Brace, Inc, Pittsburgh, PA.

Submitted April 1, 2002; accepted in revised form February 20, 2003.

prediction of healing rates and evaluation of treatment.[7,9-12] Therefore, many previous attempts have been made to characterize and quantify tissue fibrosis, including histologic examination and weighing of biopsy specimens,[13] semiquantitative clinical assessments (palpation/pitting) with subsequent grading of the tissue response,[14,10] and the use of tonometers/durometers to acquire force/displacement data (indentometry).[10,15-21] Medical imaging techniques, such as computed tomography (CT), ultrasonic elasticity imaging (elastography), and magnetic resonance imaging (MRI) have also been used.[22-36] However, these efforts have failed to produce a clinically practical, noninvasive method to measure the effects of fibrosis on the elastic and nonlinear, time-dependent tissue responses.

Figure 1.
LIPODERMATOSCLEROSIS WITH FIBROSIS, ULCERATION, AND HYPERPIGMENTATION

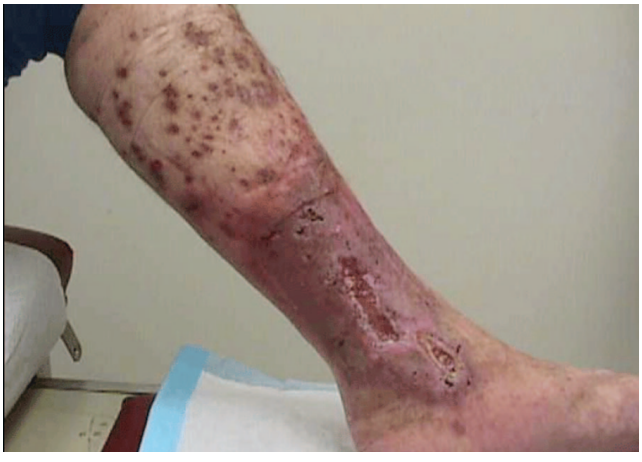

Figure 2.
CT AXIAL MID-CALF IMAGE

The bulk thickness measurement is 97 mm.

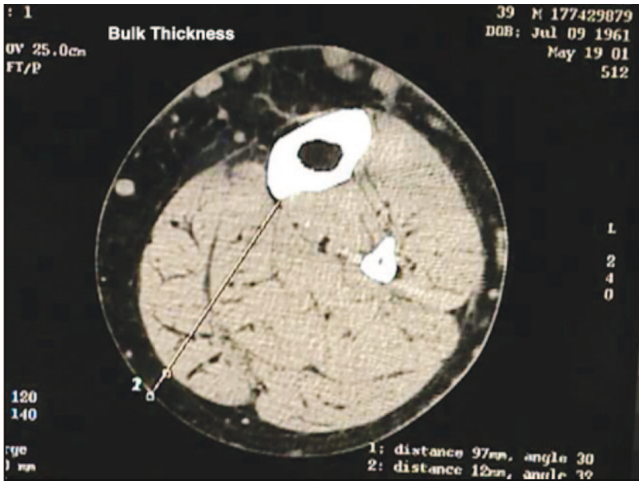

SOFT TISSUE MODELING

Human soft tissue consists of a variety of macro and molecular structures with widely varying individual properties. Mechanical properties are influenced by the unique geometry and composition of the tissue, as well as by the macromolecular structure of the tissue's extracellular matrices. Although the individual properties of soft tissue may vary, similarities are exhibited by its nonlinear, viscoelastic behaviors, including preconditioning, hysteresis, stress-relaxation, and creep.

Many theoretical models have been developed to describe soft tissue mechanical responses. The biomechanics literature is replete with studies of the material properties of soft tissue, most of which have consisted of in vitro tensile tests. However, the in vivo mechanical behavior of the skin and soft tissue is most commonly measured using compressive loading (indentometry). Over the years, several generations of indentometry devices have been used to study soft tissue responses to loading under a variety of conditions.[37-42] These studies sought to obtain tissue deformation characteristics from which estimates of lower extremity bulk tissue properties could be derived and subsequently used for finite element analysis.[38,43-45] These studies demonstrated that in addition to exhibiting stress-relaxation, human bulk tissue responses to compressive loading are nonlinear, time-dependent, and may vary as a function of strain rate, state of muscle activity, and/or subject posture.

Valid characterization of tissue properties requires a model that accounts for both the nonlinear, stress-relaxation, and elastic characteristics of the tissue. The quasi-linear, viscoelastic (QLV) model proposed by Fung incorporates these features.[46] However, until recently, limitations in accurately measuring time-dependent tissue responses and changes in the bulk tissue thickness during deformation prevented the ready application of Fung's model. The combination of ultrasound technology with indentometry has provided a means of overcoming these limitations. Ultrasound has been successfully used to monitor the changes in tissue deformation over time. Rather than using the surface displacement immediately beneath the indenter as a measure of deformation, ultrasound reflection permits a more direct measurement of the change in overall (bulk) tissue thickness.[44,47,48]

To date, only a limited number of studies have been performed using the ultrasound indentometry method. Selected tissues that have been evaluated include the buttocks,[49] lower limb,[41,50] and the plantar surface of the foot.[51,52] Comparative analyses have been used to examine differences between

apparently healthy tissue and that of diabetic patients and spinal cord-injured individuals at high risk for pressure ulcers. No biomechanical studies have been performed to quantify both the elastic and time-dependent characteristics of LDS venous-insufficient tissue.

COMPUTED TOMOGRAPHY

In recent years, the evolution of imaging techniques has extended the role of CT and MRI to examination of the microcirculation and soft tissue of the extremities. CT is the generally accepted standard for quantifying soft tissue density.[53] It may also be used to characterize the presence and severity of fibrosis and/or dermal thickening, and the appearance of suprafascial and subfascial tissue compartments. These parameters may be obtained from a single axial slice through the mid-calf with attenuation levels chosen to examine fat and muscle content[34] (Figure 2).

The use of CT to examine the fibrotic soft tissue of the extremities has been limited to research efforts because its lack of portability and cost make it impractical for use in the field. In the present study, CT served as the reference for quantifying tissue density and provided descriptive measures of fibrosis to which the parameters obtained from ultrasound indentometry were compared. Therefore, associations found between the CT descriptive and quantitative measures and the ultrasound indentometry parameters would support the validity of the ultrasound indentometry method.

Using a novel ultrasound indentometry method, the investigators aimed to quantify the mechanical properties of mediposterior bulk calf tissue in patients with LDS venous-insufficient tissue and individuals with apparently healthy tissue. A secondary aim was to identify the parameters with the greatest clinical relevance and potential for use in subsequent studies.

METHODS

Soft tissue indentation apparatus

An indentation apparatus was designed and constructed to obtain biomechanical measures of soft tissue (Figure 3). The apparatus consisted of a Blatek (State College, PA) 3.5 MHz ultrasound transducer aligned with a force sensor and an electromechanical linear actuator. The ultrasound transducer was located at the end of a 25-mm diameter probe and served as the indenter. Tissue thickness and deformation measures were determined from the A-mode ultrasound echo signal. A strain gauge cantilever beam was connected in series with the ultrasound transducer to record the force response of the tissue.

Control of the linear actuator was achieved using a CYDIO96 digit I/O interface device (CyberResearch Inc, Brandford, CT). The linear actuator could accommodate stepping rates to a maximum of 8 mm/second and indentation to 15 cm; however, the actual speed in this study was 2 mm/second and the maximum indentation was 2.4 cm. Vertical positioning of the sensor was achieved by means of a manually controlled scissors jack.

Using LabVIEW 5.0 (National Instruments, Austin, TX), software was developed to display the real-time ultrasound echoes, corresponding tissue deformations, and force measures. A 100 MHz, 8-bit Compuscope 250 card (GaGe, Lachine, CA) was used to collect and digitize ultrasound echoes and a

Table 1.
SUBJECT CHARACTERISTICS

Characteristic	LDS Group (n = 9)	Non-LDS Group (n = 9)
Age (years)		
Mean	60.4	48.3
SD	18.9	7.5
Range	40-85	37-60
Sex		
Female	5	5
Male	4	4
Race		
White	8	7
Nonwhite	1	2
Years with disease		
Mean	14.2	0
SD	11.06	0
Range	1.5-30+	0

SD = standard deviation

Table 2.
CEAP CLASSIFICATION OF CHRONIC VENOUS DISEASE—CLINICAL FINDINGS

Class	Definition
0	No visible or palpable signs of venous disease
1	Telangiectases or reticular veins
2	Varicose veins
3	Edema
4	Skin changes ascribed to venous disease (pigmentation, venous eczema, lipodermatosclerosis)
5	Skin changes (as defined above) in conjunction with healed ulcer
6	Skin changes (as defined above) in conjunction with active ulcer

Note: The presence or absence of symptoms such as pain or aching is denoted by the addition of "S" for symptomatic or "A" for asymptomatic to modify the class category.

Figure 3.
ULTRASOUND LOWER EXTREMITY TISSUE INDENTER

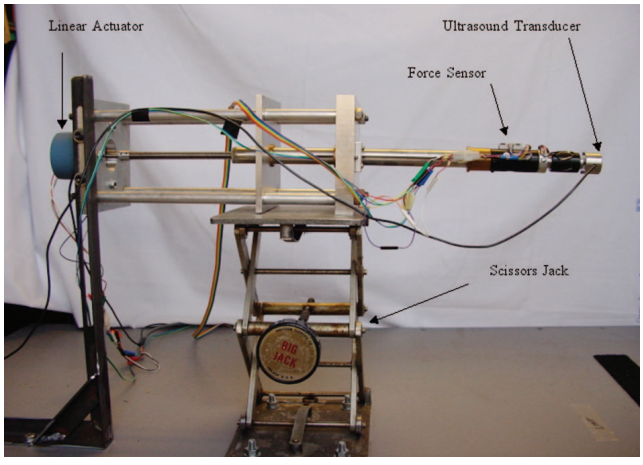

Figure 4.
ULTRASOUND ECHOES

Tissue thicknesses were derived from the echoes as follows: $[t_2 - t_1 = t_3]$, where t_2=bulk; t_1=fat; t_3=muscle, and sampling frequency = 25 MHz.

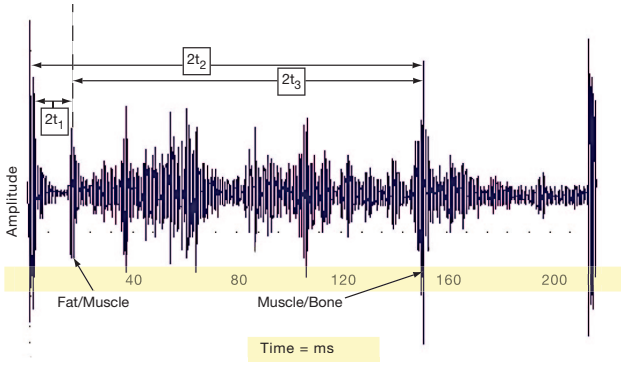

DAP 1200e (National Instruments, Austin, TX) data acquisition processor was used to obtain force measures. Data were recorded and saved to a computer file for off-line analysis. The bulk thickness of the tissue was calculated from the speed of the emitting ultrasound pulse and the time lapsed until the echoes returned to the sensor. For ease of calculation, the bulk tissue sound velocity was assumed to be 1495 m/second, the average of the velocities through fat and muscle (1450 m/second and 1540 m/second). Using the developed software, a pair of cursors could be set to automatically track the changes in the position of the echo peaks associated with the fat/muscle and muscle/bone interfaces relative to the deflection from the initial ultrasound emission. Therefore, changes in deformation could be obtained during indentation (Figure 4).

Subject recruitment

Nine subjects ages 48.3 ± 7.5 years with apparently healthy tissue (non-LDS group) and 9 subjects ages 60.4 ± 18.9 years with lipodermatosclerositc tissue (LDS group) participated in the study. In the LDS group, the mean number of years from onset of the disease to the time of the study ranged from 1.5 years to 30+ years, with a mean duration of 14.2 years (Table 1).

Figure 5.
CT FIBROSIS RATING SCALE

The scale rates fibrosis from 0 to 3, as follows: 0=none, 1=slight, 2=moderate, 3=severe.

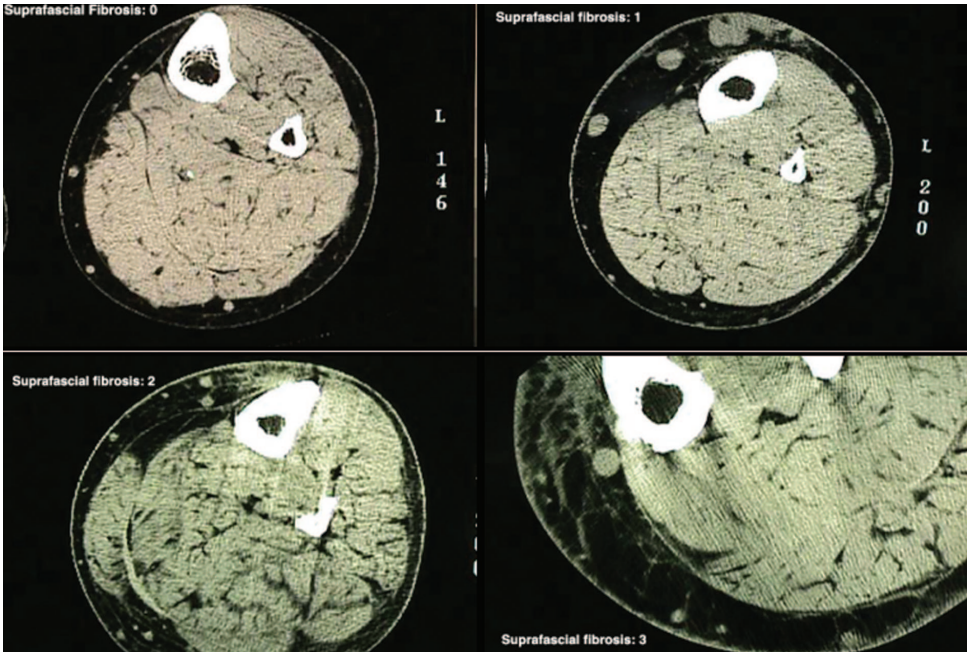

Subjects had none of the following conditions: diabetes, significant arterial disease (no ankle-brachial index less than 0.8), connective tissue disease, previous major venous surgery in either leg (nothing greater than below knee sclerotherapy or local stab avulsions), lymphoma or previous irradiation of regional lymph nodes, lymphedema, lipedema, evidence of malignant etiology to any existing ulcer(s), and no scars or current tissue injury at the loading site. In addition, all subjects in the LDS group presented with clinical findings described by CEAP classes 4, 5, or 6[54] (Table 2) and were recruited from the University of Pittsburgh Medical Center (UPMC) Wound Healing/Limb Preservation Clinic (Tables 1 and 2).

Testing protocol

For each subject, the testing period lasted 2 to 3 hours and consisted of a unilateral lower extremity CT scan of the midcalf followed by ultrasound indentometry. Before the CT procedure, the tissue indentation site was marked on the test leg. A line was drawn on the medial lower leg in the transverse plane at a point 50% to 70% of the distance from the medial malleolus to the tibial tuberosity and greater than or equal to 5 cm from the edge of any existing wound. With the subject's calf muscle contracted, a line was drawn over the medial head of the gastrocnemius muscle orthogonal to the first. The intersection of these lines marked the indentation site. A marking bead was temporarily fixed over the site to align the first CT axial slice. Three contiguous axial slices, each 3 mm thick, were obtained, with the highest centered over the marking bead. The exams were interpreted by a board-certified radiologist, who was blinded to all subject identification and to the results of the indentometry. The following 5 CT parameters were obtained for each subject: (1) suprafascial compartment density (skin and subcutaneous tissue) expressed in Hounsfield units (HU); (2) subfascial density (fascia and muscle tissue) expressed in HU; (3) thickness ratio (the ratio of suprafascial to subfascial compartment thickness); (4) dermal thickening (presence or absence); and (5) a suprafascial compartment fibrosis rating (0 = none, 1 = slight, 2 = moderate, 3 = severe) (Figure 5).

Ultrasound indentometry was performed immediately following the CT exam. During the indentation procedure, the subject was in a sitting position, with knees flexed to approximately 90 degrees, ankles

Table 3.
CENTRAL TENDENCY, POWER, AND SAMPLE SIZE

Parameter	N*	Mean Median Mode	SD	Power	Sample Size
Suprafascial density	18	-95.16	18.88	5%	>1000
Subfascial density	18	36.42	15.65	76%	10
Thickness ratio	18	0.15	0.07	76%	10
Fibrosis rating	18	Median 1	NA	80%	9
Dermal thickening	18	Mode 0	NA	NA	NA
τ_1	17	4.16	2.45	5%	>1000
τ_2	17	1.97	1.06	48%	20
k	17	0.0392	0.01	70%	12
A	17	5.24	4.14	31%	30
B	17	0.11	0.05	8%	270
E	17	15.82	8.96	100%	3

* N = 17 as QLV data on 1 non-LDS subject was lost during computer malfunction.
SD = standard deviation; NA = not applicable

Table 4.
GOODNESS OF FIT FOR ULTRASOUND INDENTOMETRY CURVE FITTING

Parameter	Mean R^2	SD	SD/Mean (%)
Effective elastic modulus: *E*	0.929	0.085	9.0
QLV elastic response: *A*, *B*	0.948	0.093	9.8
Reduced relaxation response: τ_1, τ_2, *k*	0.900	0.081	8.9

SD = standard deviation

Table 5.
RELIABILITY OF ULTRASOUND INDENTOMETRY METHOD AND CT FIBROSIS RATINGS

Parameter	N	Statistic	Value	95% CI
τ_1	14	ICC	0.356*	0.027 –0.688
τ_2	14	ICC	0.674*	0.392 – 0.868
k	14	ICC	0.641*	0.347 – 0.852
A	15	ICC	0.004	-0.24 – 0.373
B	15	ICC	0.338*	0.021 – 0.665
E	14	ICC	0.883*	0.741 – 0.957
Fibrosis rating	25**	kW	0.930*	NA

* Indicates that ICC value is significantly different from zero.
** Indicates use of additional pilot subjects' data to determine reliability.
CI = confidence interval; NA = not applicable

neutral, and the tissue site directly in line with the indenter (Figures 6a and 6b). To prevent movement, the test limb was secured to the platform via a custom brace and further restraint was provided for the upper legs and body. The indentation procedure began with the advancement of the probe until contact between the sensor and the indentation site was achieved (Figure 6c).

To precondition the tissue, cyclic loading was performed for 3 minutes at a rate of 2 mm/second to a maximum depth equal to 20% of the bulk tissue thickness (range = 1.26 to 2.42 cm). Preconditioning of the tissue prior to compressive loading has been shown to increase the linearity and reliability of the data.[41,49,50] After preconditioning the tissue, 3 ultrasound indentometry trials were performed at the same speed and compression depth as during the preconditioning period. Each trial consisted of advancing the probe to the prescribed depth, then holding the indentation for 5 minutes. A 3-minute recovery period followed each trial. Because movement artifact was a significant problem during the hold phase of each trial, some subjects were asked to perform additional trials in an attempt to obtain 3 clean trials. Regardless of the quality of the recorded stress-response curve, subjects performed a maximum of 5 trials.

Derivation of tissue mechanical properties

• ***Fung's Quasi-linear Viscoelastic (QLV) Model.*** According to the QLV model, the tissue's stress at time *t, T(t),* is dependent on both its stress history and instantaneous elastic response. That is,

(1.0) $$T(t) = \int_{-\infty}^{t} G(t-\tau)\frac{\partial T^e(\varepsilon)}{\partial \varepsilon}\frac{\partial \varepsilon}{\partial \tau}d\tau$$

where, *G(t),* the reduced relaxation function, is given by

(1.1) $$G(t) = \frac{1 - k\gamma - k\ln\left(\frac{t}{\tau_2}\right)}{1 + k\ln\left(\frac{\tau_2}{\tau_1}\right)}$$

and, $T^e(\varepsilon)$, the elastic response, is given by

(1.2) $$T^e(\varepsilon) = A\left(e^{B\varepsilon} - 1\right)$$

The parameters, k, τ_1, τ_2, A, and B may be derived by curve fitting the experimental data to the QLV model. A typical stress response for indentation is shown in Figure 7. The parameters A and B characterize the shape of the indentation phase in the stress response. A corresponds to the initial slope of the stress-time curve and B corresponds to the rate of change of the curve. Parameter k represents the amplitude of the total stress-relaxation occurring in the hold phase, while τ_1 and τ_2 represent the initial (fast) and delayed (slow) rates of stress-relaxation during the hold phase.

• ***Hayes' Effective Elastic Modulus Model.*** A sixth parameter, the effective elastic modulus,[55,56] was determined from the

Figure 6a.
TISSUE SITE

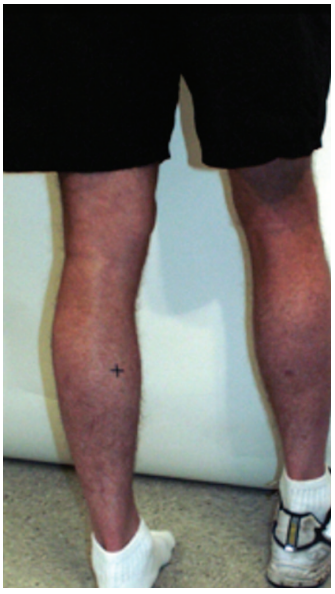

Figure 6b.
SUBJECT TEST POSITION

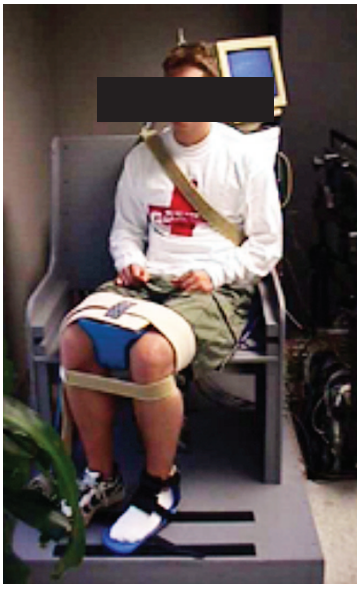

Figure 6c.
INDENTER CONTACT WITH SKIN

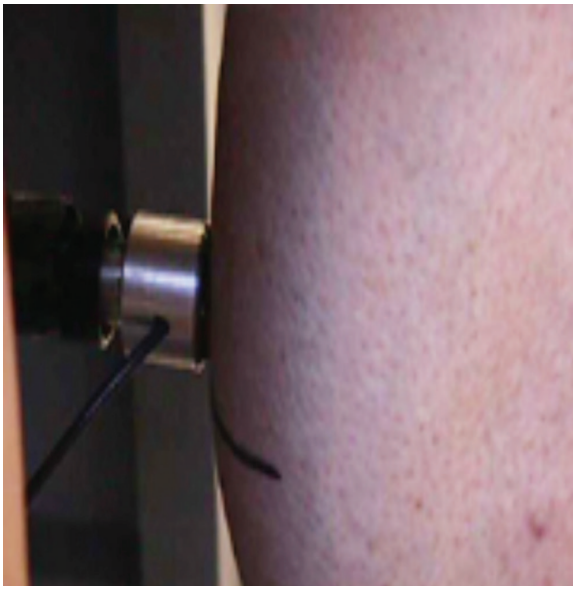

Table 6.
SIGNIFICANT LDS VS NON-LDS GROUP DIFFERENCES

Parameter	Statistic	N		Mean		SD		*P* Value
		LDS	Non-LDS	LDS	Non-LDS	LDS	Non-LDS	
k	*t* test	8	9	0.05	0.03	0.013	0.011	.020
E	*t* test	8	9	22.36	10.01	3.6	3.9	.004
Subfascial density	Mann-Whitney test	9	9	27.65	45.28	16.6	8.3	.006
Thickness ratio	*t* test	9	9	0.19	0.11	0.06	0.06	.015
Fibrosis rating	Mann-Whitney test	9	9	1.67	0.44	1.11	0.53	.019
Dermal thickening	chi-square test	9	9	4.00	0.00	NA	NA	.018

$\alpha = 0.05$
SD = standard deviation; NA = not applicable

experimental data. The effective elastic modulus, *E,* describes the approximate linear elastic response of the tissue and is represented by the solution to the Hayes et al[55] analysis of an indention to an infinite elastic layer by a rigid cylindrical indenter. Hayes et al considered the indentation mechanics of a homogenous, isotropic, infinite elastic layer bonded to a rigid half-space as a model for the layered geometry of cartilage and subchondral bone.[55] Using this analysis, a linear elastic shear modulus was determined for articular cartilage in response to indentation. More recently, this method has been adopted for analysis of the elastic properties of lower limb[41,50,57] and plantar soft tissue.[52] In these investigations, the elastic layer corresponded to bulk soft tissue, and the rigid half-space, to the underlying bone. These studies determined that *E* could simply and effectively describe the elastic properties of lower-limb soft tissue. In the present study, *E* was included for comparison with the elastic response derived via QLV modeling. *E*, the effective elastic modulus, represents the maximum slope of the stress-strain curve, or the mean ratio of load to deformation, and is given by:

(2.0) $$E = \frac{\left(1-\nu^2\right)}{2ak(\nu, a/h)}\frac{P}{w}$$

where *h* is the tissue thickness, *a* is the indentor radius, and *k* is a scaling factor dependent on *v,* Poisson's ratio, and the ratio of the indenter radius to the tissue thickness, *a/h. P/w* is the ratio of the applied load to the indentation depth. Poisson's ratio was assumed to be constant at 0.45. Because *a* and *v* are constants, equation (2.1) can be rewritten as:

(2.1) $$E = \frac{1}{K(h)}\frac{P}{w}$$

where *K*(*h*) with a unit of length is a factor dependent only on the thickness of the soft tissue, *h*. Using the value of *k* (*a/h, v*) proposed by Hayes et al,[55] the relationship between *K*(*h*) and tissue thickness (*h*) can be derived. *E* then represents an approximation of the slope of the stress-strain curve.

Data reduction and analyses

• ***General.*** All statistical tests were performed at $\alpha = 0.05$ using SamplePower, Release 1.20 (SPSS Inc, Chicago, IL). Although a number of comparisons were made between the LDS and control group, neither Bonferroni's correction nor any other correction was used to reduce Type I error. This decision was made a priori and justified by the preliminary nature of the study and the small sample size. The symmetry of the distribution of each parameter was evaluated before analysis to ensure appropriate use of a parametric or nonparametric statistical test.

• ***Curve fitting.*** To curve fit the raw data for the elastic and relaxation portions of the stress-response curve, a macro was created to find the maximum point in the curve. All data points located before this point represented the elastic response (from which parameters A, B, and E were derived); those after represented the relaxation response (from which the parameters *k,* τ_1, and τ_2 were derived). The experimental elastic data were then further reduced by selecting the points with loads greater than 0.5 Newtons (N) and less than 75% of the peak force value for analyses.[41,50] The data were rescaled assuming 0.5 N to represent the initial state, and a dimensional analysis converted the force data to pascals. The strain was then calculated from the ultrasound echoes (strain=[L-Lo]/Lo) and Microsoft Excel was used to calculate the effective elastic modulus according to equations 2.0 and 2.1. For computation of the QLV elastic parameters *A* and *B*, Mathematica 4.0 software was used to perform nonlinear regression analysis according to Woo's equation (1.2).[43]

To curve fit the raw data for the relaxation portion of the response, a macro was used to find the maximum and minimum points on the curve and to normalize the data by dividing all of the points by the maximum point value. A 3-point moving average was used to smooth the data. Mathematica 4.0 was then used to solve for parameters k, τ_1, and τ_2 using nonlinear regression analysis according to equation 1.1.[43,56] All parameters were derived from the best fit of the experimental data to their respective linear or nonlinear curves. The accuracy of curve fitting for every data set was evaluated using the coefficient of determination for curve fitting (R^2)[58] by equation:

$$(3.0) \quad R^2 = \frac{\text{Total Sum of Squares} - \text{Residual Sum of Squares}}{\text{Total Sum of Squares}}$$

Postdata reduction examples of curve fitting for the QLV elastic and reduced relaxation responses and the effective elastic modulus are shown in Figures 8a, 8b, and 8c.

Validity of the QLV model

The validity of the QLV reduced relaxation parameters, k, τ_1, and τ_2, and the elastic response parameters, A and B, were evaluated for the tissue site (medialposterior calf tissue) by performing a confirmation test according to procedures described previously by Woo.[43] The parameters extracted from the experimental data were used to predict a curve representing tissue behavior in response to the previously described cyclic loading. Experimental data were also obtained from a second cyclic loading period using a different indentation speed, compression depth, and hold period. The curve predicted by the parameters derived from the initial loading was then compared with the experimental data from the second loading protocol (Figure 9). A small mean square error between the predicted and actual response would confirm the validity of the QLV model for this tissue site and was evaluated by equation as follows:

$$(4.0) \quad MSE = (\Sigma(P_p(i)-P_a(i))^2/\ \Sigma(P_a(i))^2)^{1/2}$$

where $P_p(i)$ is the predicted force and $P_a(i)$ is the experimentally measured force.

Reliability

The intrarater reliability of the fibrosis rating scale was established with pilot data using a weighted kappa, incremental scale (0 = none, 1 = slight, 2 = moderate, 3 = severe).[58] The CT slices representing the 4 rating categories shown in Figure 5 were subsequently used as a guide to increase intrarater reliability in the actual study.

The repeatability of the ultrasound indentometry instrument in obtaining the 6 tissue response parameters for medioposterior calf tissue was estimated using the intraclass correlation coefficient (3,1). Median values of the curve-fit parameters were computed and outliers were dropped by visual inspection of the values and the stress-response curves. Of the total number of trials performed for 18 subjects, 18.8% of the data were dropped after visual inspection. Only subjects with 3 clean trials were included in the reliability analyses. The data were dropped from both groups equally for the relaxation parameters. There were slightly more outliers for the elastic parameters among the LDS group due to slight slippage at the skin-indenter interface in 2 individuals with significant muscle atrophy at the test site.

Table 7.
SIGNIFICANT CORRELATIONS BETWEEN CT AND QLV PARAMETERS

	Suprafascial Density	Suprafascial Density	Fibrosis Rating	Dermal Thickening
B	rho = - 0.608		rho = - 0.471	rho = - 0.453
	0.005*		0.028*	0.034*
E		rho = - 0.510	rho = 0.575	rho = 0.481
		0.018*	0.008*	0.025*

*Statistically significant correlation at a = 0.05; rho = Spearman rank correlation

Associations among parameters

The Pearson product moment correlation coefficient was used to evaluate correlations of continuous variables. The Spearman rank correlation coefficient was used for correlations of nonparametric data. Scatter diagrams were constructed for all correlations to determine linearity prior to analyses.

Group differences

Either the independent t test for normal distributions with interval ratio scales or the chi-square test for dichotomous data was used to evaluate group differences. The Mann-Whitney test was used in comparing 2 independent ordinal data (fibrosis rating) or skewed interval data.

Power analyses and determination of sample size

Because the ultrasound indentometry method had not previously been used to extract QLV parameters for the medioposterior calf in this population, and knowledge of the statistical characteristics of these parameters is limited, accurate power analyses were not possible a priori.

RESULTS

Equivalence between groups demographic data

The data were analyzed for group equivalence on demographic characteristics. No statistically significant differences were found between the LDS and non-LDS groups in age, sex, or race.

Central tendency and power analyses

Measures of central tendency and variability are found in Table 3. None of the parameters displayed kurtotic distributions, but 3 parameters were skewed (subfascial density, *A*, and *B*). Power analyses were subsequently conducted for all parameters used in evaluating between group differences. Sample sizes were then projected, based on the number of subjects required per group to achieve a power of 80% with 1-tailed test, $P < .05$ (Table 3).

Curve fitting

The mean coefficient of determination for curve fitting (R^2) for the QLV elastic and reduced relaxation responses and the effective elastic response are summarized in Table 4.

Curve fitting the QLV model to experimental data yielded R^2 greater than 0.90, with the mean coefficient of variation (standard deviation [SD]/mean) for each parameter less than 10%. This level of accuracy compares favorably with data obtained from normal buttocks tissue in previous experiments where the elastic response R^2 was greater than or equal to 0.90 and the coefficient of variation was less than or equal to 17%.[49] As previously explained, 2 different models were used to examine the elastic response to deformation. The R^2 value for the effective elastic modulus, *E*, was 0.929 (SD = 0.085). A similar fit, 0.948 (SD = 0.093), was found for the QLV elastic response parameters *A* and *B*.

Figure 7.
TYPICAL STRESS RESPONSE FOR AN INDENTATION TRIAL

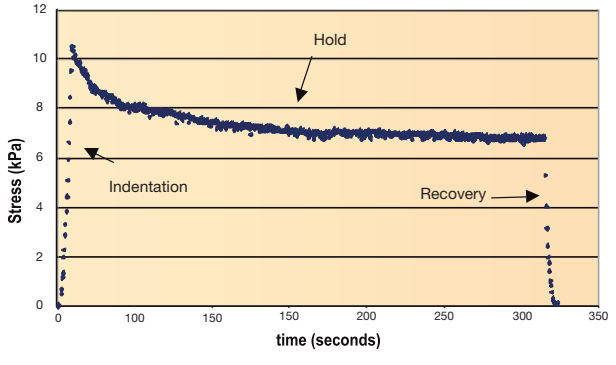

Validity of the QLV model

The error between the predicted and experimental values for the confirmation testing was small (MSE = 12.7%; Figure 9). This compares favorably with the values reported by Wang (MSE = 20%)[49] and confirms the validity of the method for use with medioposterior calf tissue.

Reliability and response stability

The reliability of the radiologist in rating fibrosis and the ICC values for each of the extracted QLV parameters (τ_1, τ_2, *k*, *A*, and *B*) and the effective elastic modulus, *E*, are shown in Table 5. Significant ICC values ranged from 0.356 (τ_1) to 0.883 (*E*). The secondary goal of this study was to identify parameters with clinical relevance and potential for use in subsequent studies. Therefore, the reliability obtained for parameters τ_2, *k*, and *E* were judged to be adequate for this purpose. The value of 0.883 obtained for *E* was close to the standard of 0.90 conventionally held for clinical reliability measures (Table 5).

Significant group differences

Group comparisons were made between the LDS and non-LDS groups on all 11 CT and QLV parameters. Statistically significant differences were found between the groups on 4 CT parameters (subfascial density, thickness ratio, fibrosis rating, and dermal thickening) and 2 QLV parameters (*k* and *E*). Table 6 summarizes these comparisons.

Significant associations were found between 4 CT parameters (suprafascial density, subfascial density, fibrosis rating, and dermal thickening) and 2 elastic QLV parameters (*B* and *E*). A summary of these correlations is shown in Table 7.

Discussion

Because no clinically practical, noninvasive method of characterizing tissue fibrosis in venous disease is currently available, this study investigated the potential use of a novel ultrasound indentometry method to quantify tissue biomechanical properties as construct variables of fibrosis. A construct variable cannot be observed directly, but is inferred by measuring correlated observable evidence. CT provided the evidence of fibrosis, and correlations between the QLV and CT parameters were sought. As the validity of the construct depends on the accuracy, reliability, and validity of the methods used to derive the biomechanical properties, the first aim of the present study was to determine the accuracy and validity of the QLV model for the selected tissue site. The reliability of the measurements obtained via the ultrasound indentometry and CT methods were also determined.

To date, only a limited number of studies have been performed using this method, and no previous studies investigat-

ing lipodermatosclerotic tissue have been reported. Being preliminary in nature, the present study has a number of limitations and the results must be interpreted accordingly.

The limits of the assumptions of 2 equations were modified, which may have resulted in error. In equation 1.1, *t* was used to fit the entire stress relaxation function (up to 300 seconds) when the expression was meant for *t* on the order of 1 second. Also, the Hayes solution to obtain *E* was applied with a deformation equal to 20% of the tissue bulk thickness when the deformation condition for the solution is described as infinitesimal. Despite these limitations, the resultant curve fitting accuracy was high and it should be noted that other investigators have used the Hayes solution with deformations as high as 30%.[41]

Limb volume increases related to the dependent position of the test leg might also have introduced error. Although fibrosis in the tissue, not edema, is the distinguishing characteristic of the severity of the disease, the macrovascular hemodynamic changes may have affected the mechanical tissue properties in some subjects more than others. Edema did not affect the CT reference parameters.

Repeated loading of the tissue site without permitting recovery to initial pretested tissue thickness may also have affected mechanical tissue properties. Preconditioning was performed to minimize this effect. To obtain precise repeated loading, the test extremity had to be immobile during the entire indentometry procedure. A 3-minute maximum recovery between trials was instituted to limit the procedure time, thereby enabling elderly subjects and subjects with active ulcers to tolerate the immobility associated with testing.

Despite these limitations, this preliminary study was successful in establishing the accuracy and validity of the QLV model for medioposterior calf tissue and in identifying acceptably reliable parameters (τ_2, *k*, and *E*) with which to characterize the stress response.

In addition to their reliability, parameters having the potential for use in further studies of this method were identified based on their ability to discriminate between apparently healthy and fibrotic, venous-insufficient tissue. In this study, construct validity depended on association with either a high CT fibrosis rating or the presence of dermal thickening.

Of the 7 parameters, parameter *k* ($P < .020$) and parameter *E* ($P < .004$) successfully discriminated between healthy and lipodermatosclerotic tissue, despite the small sample size and the limitations of the indenter. Because parameter *E* was significantly correlated with both CT fibrosis rating ($P < .008$) and the presence of dermal thickening ($P < .025$), it demonstrated the greatest construct validity.

Based on more recent reports of lymphatic and microcirculatory changes associated with chronic venous disease,[34,59,60] the presence of dermal thickening and the fibrosis rating may be considered valid descriptors of tissue fibrosis. Soft tissue changes in the advanced stages of chronic venous disease may be consistent with those of lymphedema, depending on the

Figure 8a.
QLV ELASTIC RESPONSE

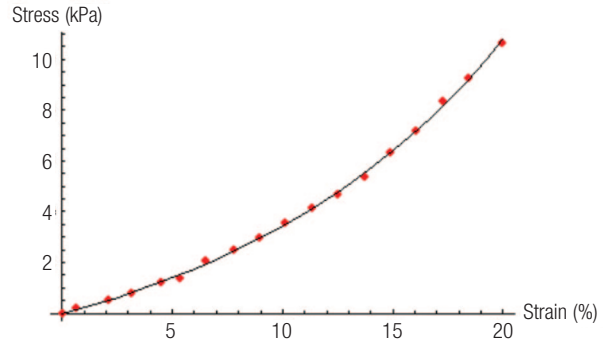

Figure 8b.
EFFECTIVE ELASTIC MODULUS

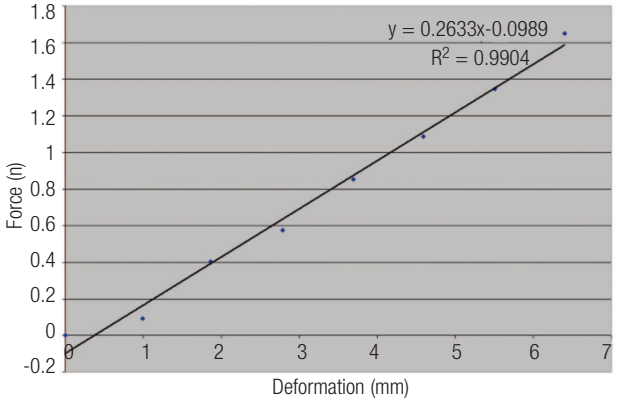

Figure 8c.
QLV REDUCED RELAXATION RESPONSE

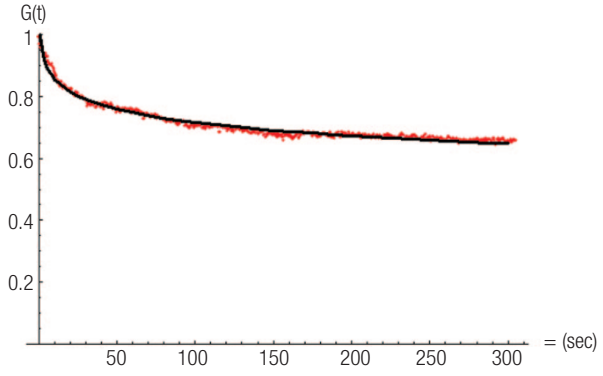

length of time since the onset of the disease and patient-specific lymphatic anatomy. The mean duration of disease for the LDS group was 14.2 years, with a range of 1.5 to 30+ years; therefore, it was expected that some lymphatic effects would be observed. Thickening of the skin is one of a number of CT findings consistently associated with lymphedema.

Dermal thickening may be due to a combination of fibrin deposition and sclerosing of the lymphatics that occurs when the lymphangitis present in the subfascial compartment spreads into the suprafascial compartment via the perforating lymphatics. Because the lymphatic vessels are contained in the same perivascular sheath as the blood vessels, this thickening may contribute to the appearance of a thickened dermal layer. According to Mallon,[59] the normally indistinct lymphatic basal lamina may be replaced by a thickened, electron-dense basal lamina. A significant difference was found between the groups for the presence of dermal thickening (P <.018).

The distinctive appearance of fibrosis in the suprafascial compartment is another finding associated with the lymphatic involvement common to later stages of chronic venous disease. Earlier stages of chronic venous disease may be characterized by edema of the muscle compartment. As the disease progresses, the perforating and suprafascial veins and lymphatics may become involved, with the subsequent accumulation of high-protein edema in the suprafascial compartment leading to fibrotic changes. In this study, the fibrosis rating scale proved extremely reliable in evaluating the severity of fibrosis in the suprafascial compartment (kW = 0.93) and the fibrosis ratings significantly differed between the 2 groups (P <.019).

Although the validity and reliability of CT density (HU) is well established, density values cannot be used to differentiate between fibrosis and normal muscle fiber. Therefore, the presence of fibrosis may be inferred only from higher density values, or a more positive HU, in the suprafascial compartment. In this study, the suprafascial mean density for the LDS group was –95.39 HU (SD = 21.3), compared with a –97.82 HU (SD = 16.5) for the non-LDS group. The slightly higher density observed for the LDS group was not significant. This lack of significance might be explained by the small sample size and within group variance.

In this study, parameter E was the only parameter to demonstrate both a significant difference between the 2 groups and a positive correlation with 2 valid CT parameters. Although parameter k also demonstrated a significant difference between the groups (P <.020), it did not significantly correlate with any CT measures. Again, this lack of significance could be due to the small sample size and within group variance.

As previously defined, parameter E, the effective elastic modulus, represents the tissue's relative stiffness; that is, the mean ratio of load to deformation. The mean elastic modulus for non-LDS subjects was 10.01 ± 3.89 kPa, with a range from 5.63 to 16.62 kPa. These values are comparable in range to those reported in similar studies[38,40,50,61] and show close agreement with the modulus of 15.5 ± 4.3 kPa reported in a similar study examining the posterior calf tissue of 8 normal males and females aged 28 ± 2 years.[50] The mean elastic modulus of the LDS subjects was 22.36 ± 8.61 kPa, with a range from 8.62 to 34.28 kPa, more than twice that of the non-LDS group. This difference was anticipated, as lipodermatosclerosis is characterized by the development of fibrous, contracted tissue.

Figure 9.
CONFIRMATION OF QLV MODEL VALIDITY FOR SELECTED CALF TISSUE

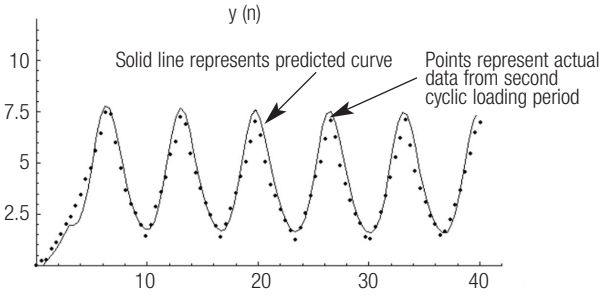

The power analyses indicate that relatively small groups (less than 30 subjects per group) would be needed to test QLV parameters k and E. With these parameters, both elastic and stress-relaxation tissue responses may be quantified.

Future studies with larger sample sizes and optimization of the protocol and prototype device, including supplemental tracking of individual fat and muscle layers, may produce more consistent echoes and eliminate much of the error variance, revealing a larger effect size for τ_1 and τ_2. Although E showed the most promise, it is premature to eliminate the QLV parameters associated with stress relaxation. Associated with viscous phenomena, these parameters may prove to be most critical in the evaluation of edematous lymphatic and venous-insufficient tissue. In other pathologic states, such as systemic sclerosis or diabetes, the tissue elastic properties may prove more relevant.

This study has successfully identified parameters derived from soft tissue mechanical responses with the potential to quantify tissue fibrosis. Further investigation is needed with a different prototype to decrease the error variance and determine the potential of all QLV parameters. ●

REFERENCES

1. De Backer G. Epidemiology of chronic venous insufficiency. Angiology 1997;48:569-76.
2. Ruckley CV. Socioeconomic impact of chronic venous insufficiency and leg ulcers. Angiology 1997;48:67-9.

3. Kerstein MD, Gahtan V. Outcomes of venous ulcer care: results of a longitudinal study. Ostomy Wound Manage 2000;46(6):22-6,28-9.
4. Burnand K, Clemenson G, Morland M, Jarrett PE, Browse NL. Venous lipodermatosclerosis: treatment by fibrinolytic enhancement and elastic compression. Br Med J 1980;280:7-11.
5. Browse NL, Burnand KG. The cause of venous ulceration. Lancet 1982;2:243-5.
6. Browse NL. The pathogenesis of venous ulceration: a hypothesis. J Vasc Surg 1988;7:468-72.
7. Kirsner RS, Pardes JB, Eaglstein WH, Falanga V. The clinical spectrum of lipodermatosclerosis. J Am Acad Dermatol 1993;28:623-7.
8. Bogensberger G, Elgart G, Froelich CW, Kirsner RS. Lipodermatosclerosis. Wounds 1999;11(Suppl A):2A-6A.
9. Nemeth AJ, Eaglstein WH, Falanga V. Clinical parameters and transcutaneous oxygen measurements for the prognosis of venous ulcers. J Am Acad Dermatol 1989;20:186-90.
10. Falanga V, Bucalo B. Use of a durometer to assess skin hardness. J Am Acad Dermatol 1993;29:47-51.
11. Margolis DJ, Kruithof EK, Barnard M, Howe K, Lazarus GS. Fibrinolytic abnormalities in two different cutaneous manifestations of venous disease. J Am Acad Dermatol 1996;34(2 Pt 1):204-8.
12. Falanga V, Fujitani RM, Diaz C, et al. Systemic treatment of venous leg ulcers with high doses of pentoxifylline: efficacy in a randomized placebo-controlled trial. Wound Repair Regen 1999;4:208-13.
13. Rodnan GP, Lipinski E, Luksick J. Skin thickness and collagen content in progressive systemic sclerosis and localized scleroderma. Arthritis Rheum 1979;22:130-40.
14. Kahaleh MB, Sultany GL, Smith EA, Huffstutter JE, Loadholt CB, LeRoy EC. A modified scleroderma skin scoring method. Clin Exp Rheumatol 1986;4:367-9.
15. Piller NB, Clodius L. The use of tissue tonometry as a diagnostic aid in extremity lymphoedema: a determination of its conservative treatment with benzo-pyrones. Lymphology 1976;9:127-32.
16. Casley-Smith JR. A tissue tonometer for use in the field. Lymphology 1985;18:192-4.
17. Kar SK, Kar PK, Mania J. Tissue tonometry: a useful tool for assessing filarial lymphedema. Lymphology 1992;25:55-61.
18. Liu N, Olszweski W. Use of tonometry to assess lower extremity lymphedema. Lymphology 1992;25:155-8.
19. Bates D, Levick J, et al. An electric tonometer to measure rate and depth of pitting in human edematous tissue. J Physiol 1993;467:16P.
20. Ferguson-Pell M, Hagisawa S, Masiello RD. A skin indentation system using a pneumatic bellows. J Rehabil Res Dev 1994;31(1):15-9.
21. Romanelli M, Falanga V. Use of a durometer to measure the degree of skin induration in lipodermatosclerosis. J Am Acad Dermatol 1995;32(1 Pt I):188-91.
22. Gamba JL, Silverman PM, Ling D, Dunnick NR, Korobkin M. Primary lower extremity lymphedema: CT diagnosis. Radiology 1983;149:218.
23. Hadjis NS, Carr DH, Banks L, Pflug JJ. The role of CT in the diagnosis of primary lymphedema of the lower limb. Am J Radiol 1985;144:361-4.
24. Krouskop TA, Dougherty DR, Vinson FS. A pulsed Doppler ultrasonic system for making noninvasive measurements of the mechanical properties of soft tissue. J Rehabil Res Dev 1987;24(2):1-8.
25. Goltner E, Gass P, Haas JP, Schneider P. The importance of volumetry, lymphscintigraphy and computer tomography in the diagnosis of brachial edema after mastectomy. Lymphology 1988;21:134-43.
26. Vaughan BF. CT of swollen legs. Clin Radiol 1990;41:24-30.
27. Bruna J. Computerized tomography, xeroradiography, lymphography and xerolymphography in diagnosis of lymphostasis. In: Olszewski W. Lymph Stasis: Pathophysiology, Diagnosis and Treatment. Boca Raton, FL: CRC Press; 1991. p 411-32.
28. Case TC, Witte CL, Witte MH, Unger EC, Williams WH. Magnetic resonance imaging in human lymphedema: comparison with lymphangioscintigraphy. Magn Reson Imaging 1992;10:549-58.
29. Duewell S, Hagspiel KD, Zuber J, von Schulthess GK, Bollinger A, Fuchs WA. Swollen lower extremity: role of MR imaging. Radiology 1992;184:227-31.
30. Fuji K. MR imaging of edematous limbs in lymphatic and nonlymphatic edema. Acta Radiologica 1994;35(Fasc 3):262-9.
31. Peschen M, Vanscheidt W, Sigmund G, Behrens JO, Schopf E. [Computerized tomography and magnetic resonance tomography studies before and after para-tibial fasciotomy.] Hautarzt 1996;47:521-5 [German].
32. Insua EM, Viano J, Martime N. Magnetic resonance imaging of peripheral lymphedema. Lymphology 1997;30:24-5.
33. Liu NF, Wang CG. The role of magnetic resonance imaging in diagnosis of peripheral lymphatic disorders. Lymphology 1998;31:119-27.
34. Marotel M, Cluzan R, Ghabboun S, Pascot M, Alliot F, Lasry JL. Transaxial computer tomography of lower extremity lymphedema. Lymphology 1998;31:180-5.
35. Werner GT, Scheck R, Kaiserling E. Magnetic resonance imaging of peripheral lymphedema. Lymphology 1998;31:34-6.
36. Ophir J, Alam SK, Garra B, et al. Elastography: ultrasonic estimation and imaging of the elastic properties of tissues. Proc Inst Mech Eng 1999;213(Pt H):203-33.
37. Ziegert J, Lewis J. In vivo mechanical properties of soft tissues covering bony prominences. J Biomech Eng 1978;100:194-201.
38. Vannah WM, Childress DS. Indentor tests and finite element modeling of bulk muscular tissue in vivo. J Rehabil Res Dev 1996;33(3):239-52.
39. Sasai S. Palpation of the skin with a robot finger: an attempt to measure skin stiffness with a probe loaded with a newly developed tactile vibration sensor and displacement sensor. Skin Res Technol 1999;5:237-46.
40. Silver-Thorn M. In vivo indentation of lower extremity limb soft tissues. IEEE Trans Rehabil Eng 1999;7:268-77.
41. Zheng Y, Mak AF. Effective elastic properties for lower limb soft tissues from manual indentation experiment. IEEE Trans Rehabil Eng 1999;7:257-67.
42. Zheng YP, Choi YK, Wong K, Chan S, Mak AF. Biomechanical assessment of plantar foot tissue in diabetic patients using an ultrasound indentation system. Ultrasound Med Biol 2000;26:451-6.
43. Woo SL, Gomez MA, Akeson WH. The time and history-dependent viscoelastic properties of the canine medial collateral ligament. J Biomech Eng 1981;103:293-8.
44. Zheng YP, Mak AF. An ultrasound indentation system for biomechanical properties assessment of soft tissues in-vivo. IEEE Trans Biomed Eng 1996;43:912-8.
45. Pathak AP. Design of rate-controlled indentor for in vivo analysis of residual limb tissues. IEEE Trans Rehabil Eng 1998;7:268-77.
46. Fung Y. Stress-Strain-History Relations of Soft Tissues in Simple Elongation. Biomechanics: Its Foundations and Objectives. Perone and Anliker, Prentice Hall, Inc; 1972.
47. Brienza D, Wang J, Ault T, Lin CT. Ultrasound measurements of tissue deformation under load. Presented at: International Conference on Wheelchairs and Seating. Dundee, Scotland; 1997.
48. Suh J, Youn I, et Kyung HS, Petrie R, Fu F. Determination of the mechanical properties of articular cartilage using a high-frequency ultrasonic indentation technique. SAME conference proceeding, 1999.
49. Wang J. Development of a Compound Ultrasound Device and In Vivo Biomechanical Assessment of Buttock Soft Tissue. Pittsburgh, PA: University of Pittsburgh; 2000.
50. Zheng YP, Mak AF. Extraction of quasi-linear viscoelastic parameters for lower limb soft tissues from manual indentation experiment. J Biomech Eng 1999;121:330-9.
51. Zheng YP, Choi Y, Wong K, Chan S, Mak A FT. Biomechanical assessment of plantar foot tissue in diabetic patients using an ultrasound indentation system. Ultrasound Med Biol 1999;26:451-6.
52. Klaesner JW, Commean PK, Hastings MK, Zou D, Mueller MJ. Accuracy and reliability testing of a portable soft tissue indentor. IEEE Trans Neural Syst Rehabil Eng 2001;9(2):232-240.
53. Shung K. X-ray: diagnostic methods. In: Shung K. Principles of Medical Imaging. San Diego, CA: Academic Press; 1992. p 39-53.
54. Kistner RL, Eklof B, Masuda EM. Diagnosis of chronic venous disease of the lower extremities: the "CEAP" classification. Mayo Clin Proc 1996;71:338-45.
55. Hayes WC, Keer LM, Herrmann G, Mockros LF. A mathematical analysis for indentation tests of articular cartilage. J Biomech 1972;5:541-51.
56. Fung Y. Biomechanics: Mechanical Properties of Living Tissues. New York: Springer-Verlag; 1993.
57. Zhang M, Zheng YP, Mak AF. Estimating the effective Young's modulus of soft tissues from indentation tests—nonlinear finite element analysis of effects of friction and large deformation. Med Eng Phys 1997;19:512-17.
58. Portney L, Watkins M. Foundations of Clinical Research: Applications to Practice. Norwalk, CT: Appleton & Lange; 1993.
59. Mallon EC, Ryan TJ. Lymphedema and wound healing. Clin Dermatol 1994;12:89-93.
60. Macdonald JM. Wound healing and lymphedema: a new look at an old problem. Ostomy Wound Manage 2001;47(4):52-7.
61. Torres-Moreno R, Morrison JB, Cooper D, Saunders CG, Foort J. A computer-aided socket design procedure for above-knee prostheses. J Rehabil Res Dev 1992;29(3):35-44.